HHS Public Access

Author manuscript

Nat Cell Biol. Author manuscript; available in PMC 2014 November 01.

Published in final edited form as:

Nat Cell Biol. 2014 May ; 16(5): 445–456. doi:10.1038/ncb2954.

Profilin-1 Phosphorylation Directs Angiocrine Expression and Glioblastoma Progression through HIF-1α Accumulation

Yi Fan[1,2], **Alka A. Potdar**[1,3], **Yanqing Gong**[4,5], **Sandeepa M. Eswarappa**[1], **Shannon Donnola**[6], **Justin D. Lathia**[1], **Dolores Hambardzumyan**[6,7], **Jeremy N. Rich**[6], and **Paul L. Fox**[1,*]

[1]Department of Cellular and Molecular Medicine, Lerner Research Institute, Cleveland Clinic, 9500 Euclid Avenue, Cleveland, Ohio, USA 44195

[2]Department of Radiation Oncology, Perelman School of Medicine, University of Pennsylvania, 3400 Civic Center Boulevard, Philadelphia, Pennsylvania, USA 19104

[3]Department of Biomedical Engineering, Case Western Reserve University, 10900 Euclid Avenue, Cleveland, Ohio, USA 44106

[4]Department of Molecular Cardiology, Lerner Research Institute, Cleveland Clinic, 9500 Euclid Avenue, Cleveland, Ohio, USA 44195

[5]Division of Translational Medicine and Human Genetics, Department of Medicine, Perelman School of Medicine, University of Pennsylvania, 3400 Civic Center Boulevard, Philadelphia, Pennsylvania, USA 19104

[6]Department of Stem Cell Biology and Regenerative Medicine, Lerner Research Institute, Cleveland Clinic, 9500 Euclid Avenue, Cleveland, Ohio, USA 44195

[7]Department of Neurosciences, Lerner Research Institute, Cleveland Clinic, 9500 Euclid Avenue, Cleveland, Ohio, USA 44195

SUMMARY

The tumor vascular microenvironment supports tumorigenesis by supplying not only oxygen and diffusible nutrients but also by secreting soluble factors that promote tumorigenesis. Here we identify a feed-forward mechanism in which endothelial cells (EC), in response to tumor-derived

*Correspondence to: Department of Cellular and Molecular Medicine, The Lerner Research Institute, Cleveland Clinic, 9500 Euclid Avenue / NC10, Cleveland, OH 44195, Tel: 216-444-8053; Fax: 216-444-9404; foxp@ccf.org.

SUPPLEMENTAL INFORMATION

Supplemental information includes Supplementary Figures 1–7, and Methods and associated references.

CONTRIBUTIONS

Y.F. designed, performed and analyzed experiments, produced figures, and wrote the initial draft of the paper. A.P. performed the gene array analysis and generated Supplementary Fig. 3. Y.G. contributed to the immunohistochemistry analysis in Fig. 5. S.D. and D.H. performed mouse GBM experiments. J.L., S.M.E., and J.N.R. helped write and edit the late drafts of the manuscript. P.L.F designed, supervised, and analyzed experiments and wrote the final draft of the manuscript.

COMPETING FINANCIAL INTERESTS

The authors declare no competing financial interests.

None of the authors have any financial conflict of interest with the information in this manuscript.

mediators, release angiocrines driving aberrant vascularization and glioblastoma multiforme (GBM) progression through a hypoxia-independent induction of hypoxia-inducible factor (HIF)-1α. Phosphorylation of profilin-1 (Pfn-1) at Tyr^{129} in EC induces binding to tumor suppressor protein von Hippel-Lindau (VHL), prevents VHL-mediated degradation of prolyl-hydroxylated HIF-1α, culminating in HIF-1α accumulation even in normoxia. Elevated HIF-1α induces expression of multiple angiogenic factors, leading to vascular abnormality and tumor progression. In a genetic model of GBM, mice with an EC-specific defect in Pfn-1 phosphorylation exhibit reduced tumor angiogenesis, normalized vasculature, and improved survival. Moreover, EC-specific Pfn-1 phosphorylation is associated with tumor aggressiveness in human glioma. These findings suggest that targeting Pfn-1 phosphorylation may offer a selective strategy for therapeutic intervention of malignant solid tumors.

Tumors are now recognized as organ-like tissues of extreme complexity[1]. Stromal cells, extracellular matrix, and soluble factors constitute the microenvironment that promotes tumor progression and metastasis, and induces therapeutic resistance[1–3]. Newly formed blood vessels deliver oxygen and nutrients to solid tumors and are crucial for their growth[4]. However, overgrown, topologically and structurally abnormal vasculature characterizes the microenvironment of most highly malignant tumors. These vessels are characterized by tortuous morphology and excessive sprouting, and are highly proliferative as well as leaky[5]. They create a host-hostile but tumor-friendly microenvironment that fuels tumor progression[6]. Therapies targeting vascular normalization recently have joined anti-angiogenesis as important strategies for reconditioning the tumor microenvironment and treating cancer[5,7].

Glioblastoma multiforme (GBM), the grade IV glioma, is among the most malignant and highly vascularized tumors, with a current median survival of about 14 months in the United States[8,9]. Most GBM tumors are refractory to conventional cytotoxic therapies, and during the past half-century there has been only limited improvement in patient treatment and prognosis[10]. GBM is distinguished by microvascular hyperplasia and extraordinary vascular abnormality of unknown etiology[8]. Anti-angiogenesis and vasculature-normalizing therapies, primarily targeting vascular endothelial growth factor (VEGF)-A and its receptors, have been developed and exploited in recent years. However, the therapeutic benefits have been small and transient, possibly due to contributions of other angiogenic factors, acquired resistance to VEGF-antagonistic treatments, and harmful treatment side-effects[11–13]. Development of strategies that target signaling molecules at points of convergence downstream of discrete angiogenic growth factor pathways may provide a solution for improving the clinical outcomes of patients with GBM.

We have recently shown that Tyr^{129} phosphorylation of profilin-1 (Pfn-1), a ubiquitously expressed actin-binding protein[14], promotes sprouting angiogenesis after ischemic injury through regulation of actin filament dynamics and increased vascular endothelial cell (EC) motility[15]. Here, we show an unexpected role of Pfn-1 phosphorylation in inducing expression of a plethora of angiogenic factors that drive vascular abnormality and GBM progression. Pfn-1 phosphorylation directs expression of endothelial angiocrines, significantly contributing to global expression of angiogenic factors in tumors. Inhibition of

this EC-specific event reduces GBM progression in a genetic mouse model that recapitulates the major features of human disease, suggesting that Pfn-1 phosphorylation represents a selective therapeutic target for treatment of GBM and other malignant tumors.

RESULTS

EC Pfn-1 phosphorylation at Tyr^{129} drives GBM progression and aberrant vascularization

Tissue array-based, multiplex analysis of human breast, liver, brain, skin, and prostate tumors revealed marked elevation of Tyr^{129}-phosphorylated Pfn-1 in multiple brain tumors types, with maximum expression in GBM (Supplementary Fig. 1). To investigate the potential role of Pfn-1 phosphorylation in tumor progression, we took advantage of our conditional, EC-specific, phos-phorylation-deficient *Tie2-Cre; Pfn1*$^{\text{flox/flox:Y129F}}$ (*Pfn1*$^{\text{Y129F}}$) knock-in mice[15], and a genetically-engineered, allogeneic mouse model of GBM that recapitulates the major features of human GBM[16]. A donor glioma was formed by stereotactic injection of DF-1 fibroblasts infected with retroviral RCAS-platelet-derived growth factor (PDGF)-B into the cortex of Nestin-tv-a *Ink4a-Arf*$^{-/-}$ *Gli-luc* donor mice (Fig. 1a). The nestin promoter drives PDGF-B expression specifically in neural stem/progenitor cells. A single-cell suspension of the glioma was injected into the cortex of *Pfn1*$^{\text{Y129F}}$ knock-in (i.e., Tie2-Cre; *Pfn1*$^{\text{flox/flox:Y129F}}$) or *Pfn1*$^{\text{WT}}$ wild-type (i.e., *Pfn1*$^{\text{flox/flox:Y129F}}$) mice recipients. Consistent with previous studies, *Pfn1*$^{\text{WT}}$ mice developed aggressive tumors exhibiting prominent vascularity with microvascular hyperplasia and extensive regions of necrosis (Fig. 1b). *Pfn1*$^{\text{WT}}$ mice became moribund after about 30 days, and all were dead by 70 days. EC knock-in of *Pfn1*$^{\text{Y129F}}$ increased median survival by about 7 days ($p < 0.05$) (Fig. 1c), nearly comparable to the 10- to 14-day increase in mouse survival by temozolomide, the current first-line standard of care for patient treatment of glioma[17,18]. Interestingly, 3 of 14 *Pfn1*$^{\text{Y129F}}$ mice survived for at least 90 days when the experiment was terminated (Fig. 1c), further suggesting the significance of this microenvironment-dependent mechanism of tumor progression.

Tumors from *Pfn1*$^{\text{Y129F}}$ knock-in mice have markedly reduced microvascular density (Fig. 1d), and the vessels exhibit morphological features typical of the vascular abnormality common in human GBM, i.e., tortuous, granular, and dilated with multi-layer wall thickening accompanied by extensive hemorrhage (Fig. 1e, f). Remarkably, blood vessels in *Pfn1*$^{\text{Y129F}}$ knock-in mice appear essentially “normalized” as evidenced by non-tortuous, thin capillary vessels with less hemorrhage. Abnormal tumor vasculature is also characterized by insufficient coverage of nascent endothelium by pericytes, which hampers vessel maturation. Defective pericyte support and structural deformity of blood vessels are associated with poor functionality of the vasculature, leading to plasma leakage and spatially heterogeneous hypoxia[19]. Defective EC Pfn-1 phosphorylation substantially increased the extent of pericyte coverage on tumor blood vessels from 56.1 ± 8.2% to 87.3 ± 6.9% (mean ± SEM, n = 5 mice, $P < 0.05$ by two-tailed unpaired *t* test, Fig. 1g), inhibited leakage of intravenous fluorescein isothiocyanate (FITC)-dextran (as shown by decreased fluorescence intensity from 473 ± 117 to 145 ± 21, mean ± SEM, n = 5 mice, $P < 0.05$ by two-tailed unpaired *t* test, Fig. 1h), and reduced intra-tumoral hypoxia as determined by Hydroxyprobe-1 Kit (as shown by decreased fluorescence intensity from 718 ± 104 to 329 ±

32, mean ± SEM, n = 5 mice, $P < 0.05$ by two-tailed unpaired *t* test, Fig. 1i), Together these results indicate an important contribution of Pfn-1 phosphorylation to vascular abnormality.

EC Pfn-1 phosphorylation at Tyr^{129} contributes to aberrant tube formation, exuberant proliferation, and monolayer hyperpermeability *in vitro*

To further investigate the EC-specific function of Pfn-1 phosphorylation, EC isolated from *Pfn1*^{WT} and *Pfn1*^{Y129F} knock-in mice were incubated with human U251 glioma cell-conditioned medium (GCM) on matrigel-coated dishes. Consistent with *in vivo* results, defective Pfn-1 phosphorylation of EC substantially reduced vessel thickening and sprouting *in vitro* (Fig. 2a). Similarly, GCM-stimulated proliferation (Fig. 2b) and monolayer permeability (Fig. 2c) was markedly reduced in *Pfn1*^{Y129F} EC. These results suggest that tumor microenvironment-dependent Pfn-1 phosphorylation drives EC over-proliferation and vascular hyperpermeability, and contributes importantly to microvascular hyperplasia during GBM progression. We previously established a role of Pfn-1 phosphorylation at Tyr^{129} in EC motility and vessel sprouting, consistent with its restricted localization at the cell leading edge during chemotaxis in response to VEGF-A[15]. Interestingly, GCM induced accumulation of Tyr^{129}-phosphorylated Pfn-1 to the perinuclear area as well as the cell leading edge in migrating EC, in contrast to its restricted localization at cell protrusion sites in the absence of GCM (Fig. 2d), possibly indicating an alternate function of Pfn-1 phosphorylation in the glioma microenvironment.

Pfn-1 phosphorylation at Tyr^{129} is critical for expression of angiogenic growth factors *in vitro* and *in vivo*

We investigated the molecular mechanism underlying Pfn-1 phosphorylation-mediated vascular abnormality. Mouse GBM with defective EC-specific phosphorylation of Pfn-1 exhibited markedly reduced expression of the angiogenic growth factors VEGF-A and basic fibroblast growth factor (bFGF) (Fig. 3a). The result suggests that expression of Pfn-1 phosphorylation-mediated EC angiocrines contribute importantly to the burden of angiogenic growth factors in GBM. The specific role of EC as growth factor source was investigated by GCM stimulation of EC isolated from mouse aorta. An angiogenesis-specific antibody array showed that GCM-induced EC expression of multiple growth factors and cytokines, including VEGF-A, VEGF-B, placenta growth factor (PlGF), heparin-binding epidermal growth factor-like growth factor (HB-EGF), and bFGF, was substantially higher in Tyr^{129} Pfn-1 phosphorylation-competent EC (Fig. 3b and Supplementary Fig. 2). The requirement for Tyr^{129} phosphorylation and GCM stimulation for enhanced expression of select targets was confirmed by immunoblot analysis (Fig. 3c). Real-time PCR revealed that regulation is primarily at the level of mRNA expression (Fig. 3d). These results suggest that the abundant vasculature in the GBM microenvironment expresses angiogenic factors at a high level in a Pfn-1 phosphorylation-dependent manner, contributing to vascular abnormality and tumor progression.

Pfn-1 phosphorylation-mediated expression of angiogenic factors requires HIF-1α

The expression of several phospho-Pfn-1-dependent factors, including VEGF-A, HB-EGF, and bFGF, is induced by the hypoxia-inducible factor (HIF)-1α transcription factor in

tumors[20,21]. Consistent with these findings, GCM stimulated HIF-1α and -2α expression, the induction of both requiring Tyr[129] Pfn-1 phosphorylation in EC (Fig. 3e). Remarkably, HIF-1α induction was observed even under normoxia, which ordinarily induces rapid ubiquitinylation and degradation. siRNA-mediated knockdown showed that HIF-1α is essential for GCM-stimulated induction of growth factors (Fig. 3f), as well as for increased EC proliferation and permeability (Fig. 3g). In contrast, HIF-2α knockdown did not appreciably inhibit growth factor expression (Fig. 3h). Transcriptome-wide analysis of tumor-derived EC shows diminished expression of multiple HIF-1α-inducible genes in Pfn-1 phosphorylation-deficient mice (Supplementary Fig. 3). These results reveal an unexpected role of Pfn-1 phosphorylation in HIF-1α–mediated expression of angiogenic factors, which might contribute to EC proliferation and vascular hyperpermeability in the glioma microenvironment.

Tyr[129]-phosphorylated Pfn-1 induces accumulation of Pro-hydroxylated HIF-1α by inhibiting VHL-mediated degradation

During normoxia, HIF-1α is subject to prolyl hydroxylation and consequent degradation mediated by tumor suppressor protein von Hippel-Lindau (VHL), thus driving low-level expression of HIF-1α in physiological conditions[22,23]. The hypoxic tumor microenvironment suppresses prolyl hydroxylation of HIF-1α and VHL binding, thereby inducing HIF-1α accumulation[24,25]. To explore the mechanism by which Pfn-1 phosphorylation induces HIF-1α in normoxia, we investigated the stimulus-dependent interactions of phospho-Pfn-1 with VHL and HIF-1α. Angiogenic growth factors expressed in human GBM, i.e., VEGF-A, PlGF, bFGF, and PDGF[26,27], stimulated phosphorylation of Pfn-1 and its interaction with VHL (Fig. 4a); particularly robust stimulation of both processes was observed with GCM. Pfn-1 bearing the Y129F mutation did not bind VHL in GCM-treated EC indicating a strict requirement for phosphorylation (Fig. 4b). Co-immunoprecipitation confirmed the GCM-stimulated interaction between endogenous Pfn-1 and VHL (Fig. 4c). Furthermore, co-localization of Tyr[129]-phosphorylated Pfn-1 and VHL was detected, primarily in the perinuclear region of GBM-stimulated EC (Fig. 4d).

To investigate direct binding of Pfn-1 to VHL, the proteins were expressed and purified, and their interaction analyzed by surface plasmon resonance (SPR) spectroscopy. Phosphorylated wild-type Pfn-1 (generated by *in vitro* incubation with lysate from GCM-activated cells or with purified Src kinase) exhibited greater affinity for VHL than the Y129F mutant (Fig. 4e and Supplementary Fig. 4). Furthermore, pre-incubation of VHL with lysate-treated Pfn-1^{WT} abrogated VHL binding to HIF-1α, whereas pre-incubation with Pfn-1^{Y129F} was ineffective, indicating that phosphorylation-dependent Pfn-1 binding to VHL prevents VHL binding to HIF-1α (Fig. 4f). Pfn-1 also interacts with G-actin in a Tyr[129]-phosphorylation-dependent manner[15]. We found that G-actin competes with VHL for Pfn-1 binding, confirming the interaction of both partners at or near the same site (Supplementary Fig. 5).

Phospho-Pfn-1 competition with HIF-1α for VHL binding might lead to constitutive expression of HIF-1α in its Pro-hydroxylated form. Indeed, GCM treatment of EC in normoxia induced HIF-1α expression to nearly the same extent as hypoxic treatment in the

absence of GCM; however, only GCM induced accumulation of Pro^{564}-hydroxylated HIF-1α (Fig. 4g). In the presence of non-phosphorylatable Pfn-1, HIF-1α was induced by hypoxia but not by GCM. Treatment of EC with the proteasome inhibitor MG-132 induced robust accumulation of HIF-1α and Pro^{564}-hydroxylated HIF-1α in both Pfn-1^{WT} and Pfn-1^{Y129F} cells, suggesting that Pfn-1 phosphorylation state does not influence prolyl hydroxylation of HIF-1α (Fig. 4h). GCM did not stimulate Pfn-1 phosphorylation or HIF-1α expression in mouse fibroblasts or GBM cells, indicating EC specificity of the pathway (Fig. 4i). Furthermore, knockdown of VHL substantially increased vessel thickening and sprouting on Matrigel and cell proliferation, and abolished the difference between Pfn-1^{WT} and Pfn-1^{Y129F} EC, consistent with an important contribution of VHL to Pfn-1 phosphorylation-mediated vascular abnormality in glioma condition (Fig. 5a–d).

To determine the *in vivo* role of this regulatory mechanism during GBM progression, Pro^{564}-hydroxylated HIF-1α was visualized in sections of mouse GBM tumors. Pro-hydroxylated HIF-1α was abundant in the tumor and co-localized almost exclusively with $CD31^+$ blood vessels (Fig. 6a, b); tumors of Pfn-1^{Y129F} mice exhibited very low-amounts of Pro-hydroxylated HIF-1α and HIF-1α (Fig. 6a–c). Similarly, human GBM specimens showed preferential co-localization of Pro-hydroxylated HIF-1α with EC, whereas total HIF-1α was distributed throughout the tissue (Fig. 6d). Together, these results reveal a non-canonical, hypoxia-independent mechanism for HIF-1α induction, by which phospho-Pfn-1-Tyr^{129} binds VHL and prevents VHL-mediated HIF-1α degradation, leading to accumulation of Pro-hydroxylated HIF-1α in EC in culture and *in vivo*, even in normoxia.

Phosphorylation of Pfn-1 at Tyr^{129} is elevated in blood vessels of human GBM tumors, and is associated with glioma grade

Pfn-1 phosphorylation was determined in human biopsy specimens during glioma progression to GBM. Elevated phospho-Pfn-1-Tyr^{129} expression was observed in Grades III and IV glioma, but not in Grades I and II (Fig. 7a). Quantitative immunofluorescence showed that Pfn-1 phosphorylation correlated with glioma grade in tumor regions and in EC (Fig. 7b, c). In all grades, phospho-Pfn-1-Tyr^{129} expression was observed almost exclusively co-localizing with $CD31^+$ blood vessels highly abundant in Grade IV (GBM) specimens (Fig. 7a, d). Moreover, essentially all blood vessels in GBM tumor were associated with phospho-Pfn-1-Tyr^{129}. Co-localization with CD144 $(VE\text{-}cadherin)^+$ vessels confirmed EC-specific Pfn-1 phosphorylation (Fig. 7e). In contrast, phospho-Akt-Ser^{473}, the critical regulatory product of PI3K activation, was more uniformly expressed, and co-localization with $CD144^+$ blood vessels was minimal. Moreover, the distribution of total Pfn-1 was uniformly expressed throughout the tissue, and in healthy brain tissue (Fig. 7f). These results further support EC-selective phosphorylation of Pfn-1 during GBM progression. Growth factor-stimulated induction of Pfn-1 phosphorylation in EC, in tandem with the consequent increase in angiocrine expression, might constitute a feed-forward loop, driving uncontrolled growth factor expression, aberrant vascularization, and consequent accelerated disease progression (Fig. 8). Knockdown of HIF-1α inhibited GCM-induced Pfn-1 Tyr^{129} phosphorylation supporting the proposed feed-forward mechanism of angiocrine production (Supplementary Fig. 6).

Pfn-1 mRNA expression correlates with poor glioma patient survival

Consistent with the role of Pfn-1 phosphorylation in glioma progression, database analysis of GBM gene expression reveals elevated mRNA encoding Pfn-1, but not other actin-binding proteins including cofilin-1, formin, fascin, and N-WASP (Supplementary Fig. 7a, b), suggesting a non-canonical function of Pfn-1 besides regulation of actin dynamics. Moreover, high Pfn-1 mRNA expression predicts poor glioma patient survival (Supplementary Fig. 7c) suggesting the possible role of Pfn-1 as a biomarker of glioma aggressiveness. However, the specific role of Pfn-1 phosphorylation in patient survival has not been investigated.

DISCUSSION

HIF-1α is a critically important transcription factor instrumental in regulating diverse cellular responses to hypoxia, inducing expression of glycolytic enzymes and multiple angiogenic growth factors that drive aberrant vascularization during tumorigenesis[6,24,25,28]. HIF-1α is upregulated in most malignant tumors, primarily by hypoxia-induced protein stabilization[25]. Here we show a non-canonical, hypoxia-independent mechanism of HIF-1α induction in EC, in which phosphorylation of Pfn-1 at Tyr^{129} inhibits VHL-mediated HIF-1α degradation by direct, competitive inhibition of VHL binding to HIF-1α. In turn, elevated HIF-1α induces expression of multiple angiogenic factors, eventually leading to aberrant vascularization and GBM progression (Fig. 8).

Phospho-Pfn-1 directs accumulation of HIF-1α even under normoxic conditions. Normoxic induction of HIF-1α by reactive oxygen species[29], PLC/PKC[30], and succinate[31,32] has been previously reported, and these agents inhibit protein hydroxylation thereby preventing recognition and degradation of HIF-1α by VHL. Likewise, human epidermal growth factor-like receptor 2 (HER2) induces HIF-1α expression in normoxia; however, the mechanism depends on increased synthesis of HIF-1α, not VHL-dependent degradation[33,34]. HER2 expression correlates with the breast cancer progression and is an important diagnostic biomarker and therapeutic target for breast cancer, but is overexpressed in only 10–15% of GBM tumors[35–37]. Here we describe a distinct, phospho-Pfn-1-driven mechanism that prevents recognition of prolyl hydroxylated HIF-1α by VHL, thereby facilitating accumulation of the modified protein in tumor EC, even in a normoxic microenvironment.

The classic role of EC is to provide physical structure that lines blood vessels, however, secretion of soluble factors by EC robustly regulates post-injury tissue regeneration and tumorigenesis[38–41]. Autocrine and paracrine effects of angiogenic growth factors, including VEGF and basic FGF, on EC contribute importantly to vascular homeostasis and angiogenesis[21,42–44]. Here, we show that expression of endothelial angiocrines driven by Pfn-1 phosphorylation significantly contributes to vascular abnormality and GBM progression. Endothelial angiocrines are a major source of angiogenic factors in GBM, likely due to prominent vascularization of the tumor. Importantly, extensive and abnormal vasculature in malignant solid tumors has been linked to resistance to radiation and chemotherapy, and poor patient outcome[6].

In more than half of the GBM patients treated with anti-VEGF therapy, a transient response, therapeutic ineffectiveness, and harmful side-effects have been observed, possibly implicating other angiogenic factors, e.g., placenta-derived, hepatocyte, and fibroblast growth factors, in therapeutic resistance[12,13,45]. Therapeutic strategies specifically targeting signaling molecules at points of convergence downstream of these diverse angiogenic growth factor pathways might prove to be more effective with lesser adverse, off-target consequences. This concept is the basis of intensive investigation of inhibitors of the pro-angiogenic PI-3-kinase/Akt pathway as therapeutic targets for GBM[10]. We have previously shown that Tyr^{129} phosphorylation of Pfn-1 is a principal component of an alternative pathway of sprouting angiogenesis that is independent of and complementary to the PI-3-kinase/Akt pathway[15]. Here, we show that Pfn-1 phosphorylation may present a critical regulatory node in EC expression of angiogenic factors, in addition to its direct stimulation of sprouting angiogenesis, both critical events in tumor vascularization. Morevoer, Pfn-1 phosphorylation is preferentially induced in the blood vessels of GBM tumors, consistent with a role in regulation of EC-derived angiocrines, in contrast to the more uniform activation of PI-3-kinase/Akt in multiple cell types. Thus, Inhibition of Pfn-1 phosphorylation may offer a selective therapeutic strategy for targeting expression of multiple angiogenic factors in tumors.

Pfn-1 is an actin-binding protein that regulates processes involved in cell propulsion including increasing G-actin availability and polymerization, as well as protease expression[46–48]. Our findings reveal an unconventional function of Pfn-1 in autocrine or paracrine signaling through HIF-1α induction and growth factor expression during GBM progression. Pfn-1 phosphorylation may have a major effect on HIF-1 stability rather than actin dynamics in glioma. Although *Tie2* robustly drives EC gene expression, the Tie2 promoter is also activated in the myeloid lineage and thus Tie2-Cre-mediated knockin of $Pfn1^{Y129F}$ might reduce Pfn-1 phosphorylation in macrophages[49,50]. Certainly tumor-associated macrophage have an important role in tumor vascularization and progression in glioma[50,51], but the contribution of macrophage Pfn-1 phosphorylation is not known.

In summary, Pfn-1 phosphorylation regulates endothelial angiocrine expression and drives aberrant vascularization and GBM progression through a hypoxia-independent HIF-1α induction mechanism. As a corollary, prevention of Pfn-1 phosphorylation might offer a selective target and strategy to inhibit endothelial angiocrine expression and normalize aberrant vasculartur, recondition the microenvironment, and improve the therapeutic window for traditional chemotherapy, for example, treatment of GBM and possibly other solid malignant tumors.

Supplementary Material

Refer to Web version on PubMed Central for supplementary material.

Acknowledgments

We are grateful to Arie Horowitz for helpful suggestions, Emilee Ritchie for technical assistance, and Judith Drazba for image analysis. This work was supported in part by National Institutes of Health grants K99 HL103792 (to Y.F.), and P01 HL029582, P01 HL076491, and R21 HL094841 (to P.L.F.).

References

1. Hanahan D, Weinberg RA. Hallmarks of cancer: the next generation. Cell. 2011; 144:646–674. [PubMed: 21376230]
2. Vaupel P, Kallinowski F, Okunieff P. Blood flow, oxygen and nutrient supply, and metabolic microenvironment of human tumors: a review. Cancer Res. 1989; 49:6449–6465. [PubMed: 2684393]
3. Joyce JA, Pollard JW. Microenvironmental regulation of metastasis. Nat Rev Cancer. 2009; 9:239–252. [PubMed: 19279573]
4. Folkman J. Tumor angiogenesis: therapeutic implications. N Engl J Med. 1971; 285:1182–1186. [PubMed: 4938153]
5. Jain RK. Normalizing tumor vasculature with anti-angiogenic therapy: a new paradigm for combination therapy. Nat Med. 2001; 7:987–989. [PubMed: 11533692]
6. Carmeliet P, Jain RK. Principles and mechanisms of vessel normalization for cancer and other angiogenic diseases. Nat Rev Drug Discov. 2011; 10:417–427. [PubMed: 21629292]
7. Weis SM, Cheresh DA. Tumor angiogenesis: molecular pathways and therapeutic targets. Nat Med. 2011; 17:1359–1370. [PubMed: 22064426]
8. Burger PC, Vogel FS, Green SB, Strike TA. Glioblastoma multiforme and anaplastic astrocytoma. Pathologic criteria and prognostic implications. Cancer. 1985; 56:1106–1111. [PubMed: 2990664]
9. Johnson DR, O'Neill BP. Glioblastoma survival in the United States before and during the temozolomide era. J Neurooncol. 2012; 107:359–364. [PubMed: 22045118]
10. Huse JT, Holland EC. Targeting brain cancer: advances in the molecular pathology of malignant glioma and medulloblastoma. Nat Rev Cancer. 2010; 10:319–331. [PubMed: 20414201]
11. Kim KJ, et al. Inhibition of vascular endothelial growth factor-induced angiogenesis suppresses tumour growth in vivo. Nature. 1993; 362:841–844. [PubMed: 7683111]
12. Batchelor TT, et al. AZD2171, a pan-VEGF receptor tyrosine kinase inhibitor, normalizes tumor vasculature and alleviates edema in glioblastoma patients. Cancer Cell. 2007; 11:83–95. [PubMed: 17222792]
13. Friedman HS, et al. Bevacizumab alone and in combination with irinotecan in recurrent glioblastoma. J Clin Oncol. 2009; 27:4733–4740. [PubMed: 19720927]
14. Witke W. The role of profilin complexes in cell motility and other cellular processes. Trends Cell Biol. 2004; 14:461–469. [PubMed: 15308213]
15. Fan Y, et al. Stimulus-dependent phosphorylation of profilin-1 in angiogenesis. Nat Cell Biol. 2012; 14:1046–1056. [PubMed: 23000962]
16. Charles N, et al. Perivascular nitric oxide activates notch signaling and promotes stem-like character in PDGF-induced glioma cells. Cell Stem Cell. 2010; 6:141–152. [PubMed: 20144787]
17. Galban S, et al. DW-MRI as a biomarker to compare therapeutic outcomes in radiotherapy regimens incorporating temozolomide or gemcitabine in glioblastoma. PLoS One. 2012; 7:e35857. [PubMed: 22536446]
18. McConville P, et al. Magnetic resonance imaging determination of tumor grade and early response to temozolomide in a genetically engineered mouse model of glioma. Clin Cancer Res. 2007; 13:2897–2904. [PubMed: 17504989]
19. Jain RK. Molecular regulation of vessel maturation. Nat Med. 2003; 9:685–693. [PubMed: 12778167]
20. Forsythe JA, et al. Activation of vascular endothelial growth factor gene transcription by hypoxia-inducible factor 1. Mol Cell Biol. 1996; 16:4604–4613. [PubMed: 8756616]
21. Calvani M, Rapisarda A, Uranchimeg B, Shoemaker RH, Melillo G. Hypoxic induction of an HIF-1α-dependent bFGF autocrine loop drives angiogenesis in human endothelial cells. Blood. 2006; 107:2705–2712. [PubMed: 16304044]
22. Schofield CJ, Ratcliffe PJ. Oxygen sensing by HIF hydroxylases. Nat Rev Mol Cell Biol. 2004; 5:343–354. [PubMed: 15122348]
23. Min JH, et al. Structure of an HIF-1α-pVHL complex: hydroxyproline recognition in signaling. Science. 2002; 296:1886–1889. [PubMed: 12004076]

24. Keith B, Simon MC. Hypoxia-inducible factors, stem cells, and cancer. Cell. 2007; 129:465–472. [PubMed: 17482542]
25. Semenza GL. Intratumoral hypoxia, radiation resistance, and HIF-1. Cancer Cell. 2004; 5:405–406. [PubMed: 15144945]
26. Plate KH, Breier G, Weich HA, Risau W. Vascular endothelial growth factor is a potential tumour angiogenesis factor in human gliomas in vivo. Nature. 1992; 359:845–848. [PubMed: 1279432]
27. Dunn IF, Heese O, Black PM. Growth factors in glioma angiogenesis: FGFs, PDGF, EGF, and TGFs. J Neurooncol. 2000; 50:121–137. [PubMed: 11245272]
28. Nyberg P, Salo T, Kalluri R. Tumor microenvironment and angiogenesis. Front Biosci. 2008; 13:6537–6553. [PubMed: 18508679]
29. Park JH, et al. Gastric epithelial reactive oxygen species prevent normoxic degradation of hypoxia-inducible factor-1alpha in gastric cancer cells. Clin Cancer Res. 2003; 9:433–440. [PubMed: 12538497]
30. Sumbayev VV. LPS-induced Toll-like receptor 4 signalling triggers cross-talk of apoptosis signal-regulating kinase 1 (ASK1) and HIF-1alpha protein. FEBS Lett. 2008; 582:319–326. [PubMed: 18155167]
31. Selak MA, et al. Succinate links TCA cycle dysfunction to oncogenesis by inhibiting HIF-α prolyl hydroxylase. Cancer Cell. 2005; 7:77–85. [PubMed: 15652751]
32. Tannahill GM, et al. Succinate is an inflammatory signal that induces IL-1β through HIF-1α. Nature. 2013; 496:238–242. [PubMed: 23535595]
33. Laughner E, Taghavi P, Chiles K, Mahon PC, Semenza GL. HER2 (neu) signaling increases the rate of hypoxia-inducible factor 1alpha (HIF-1α) synthesis: novel mechanism for HIF-1-mediated vascular endothelial growth factor expression. Mol Cell Biol. 2001; 21:3995–4004. [PubMed: 11359907]
34. Li YM, et al. A hypoxia-independent hypoxia-inducible factor-1 activation pathway induced by phosphatidylinositol-3 kinase/Akt in HER2 overexpressing cells. Cancer Res. 2005; 65:3257–3263. [PubMed: 15833858]
35. Koka V, et al. Role of Her-2/neu overexpression and clinical determinants of early mortality in glioblastoma multiforme. Am J Clin Oncol. 2003; 26:332–335. [PubMed: 12902879]
36. Potti A, et al. Determination of HER-2/neu overexpression and clinical predictors of survival in a cohort of 347 patients with primary malignant brain tumors. Cancer Invest. 2004; 22:537–544. [PubMed: 15565811]
37. Haynik DM, Roma AA, Prayson RA. HER-2/neu expression in glioblastoma multiforme. Appl Immunohistochem Mol Morphol. 2007; 15:56–58. [PubMed: 17536308]
38. Ding BS, et al. Inductive angiocrine signals from sinusoidal endothelium are required for liver regeneration. Nature. 2010; 468:310–315. [PubMed: 21068842]
39. Ding BS, et al. Endothelial-derived angiocrine signals induce and sustain regenerative lung alveolarization. Cell. 2011; 147:539–553. [PubMed: 22036563]
40. Muramatsu R, et al. Angiogenesis induced by CNS inflammation promotes neuronal remodeling through vessel-derived prostacyclin. Nat Med. 2012; 18:1658–1664. [PubMed: 23042236]
41. Lu J, et al. Endothelial Cells Promote the Colorectal Cancer Stem Cell Phenotype through a Soluble Form of Jagged–1. Cancer Cell. 2013; 23:171–185. [PubMed: 23375636]
42. Lee S, et al. Autocrine VEGF signaling is required for vascular homeostasis. Cell. 2007; 130:691–703. [PubMed: 17719546]
43. Seghezzi G, et al. Fibroblast growth factor-2 (FGF-2) induces vascular endothelial growth factor (VEGF) expression in the endothelial cells of forming capillaries: an autocrine mechanism contributing to angiogenesis. J Cell Biol. 1998; 141:1659–1673. [PubMed: 9647657]
44. Butler JM, Kobayashi H, Rafii S. Instructive role of the vascular niche in promoting tumour growth and tissue repair by angiocrine factors. Nat Rev Cancer. 2010; 10:138–146. [PubMed: 20094048]
45. Kreisl TN, et al. Phase II trial of single-agent bevacizumab followed by bevacizumab plus irinotecan at tumor progression in recurrent glioblastoma. J Clin Oncol. 2009; 27:740–745. [PubMed: 19114704]

46. Fan Y, Gong Y, Ghosh PK, Graham LM, Fox PL. Spatial coordination of actin polymerization and ILK-Akt2 activity during endothelial cell migration. Dev Cell. 2009; 16:661–674. [PubMed: 19460343]

47. Janke J, et al. Suppression of tumorigenicity in breast cancer cells by the microfilament protein profilin 1. J Exp Med. 2000; 191:1675–1686. [PubMed: 10811861]

48. Ding Z, Gau D, Deasy B, Wells A, Roy P. Both actin and polyproline interactions of profilin-1 are required for migration, invasion and capillary morphogenesis of vascular endothelial cells. Exp Cell Res. 2009; 315:2963–2973. [PubMed: 19607826]

49. Venneri MA, et al. Identification of proangiogenic TIE2-expressing monocytes (TEMs) in human peripheral blood and cancer. Blood. 2007; 109:5276–5285. [PubMed: 17327411]

50. De Palma M, et al. Tie2 identifies a hematopoietic lineage of proangiogenic monocytes required for tumor vessel formation and a mesenchymal population of pericyte progenitors. Cancer Cell. 2005; 8:211–226. [PubMed: 16169466]

51. Pyonteck SM, et al. CSF-1R inhibition alters macrophage polarization and blocks glioma progression. Nat Med. 2013; 19:1264–1272. [PubMed: 24056773]

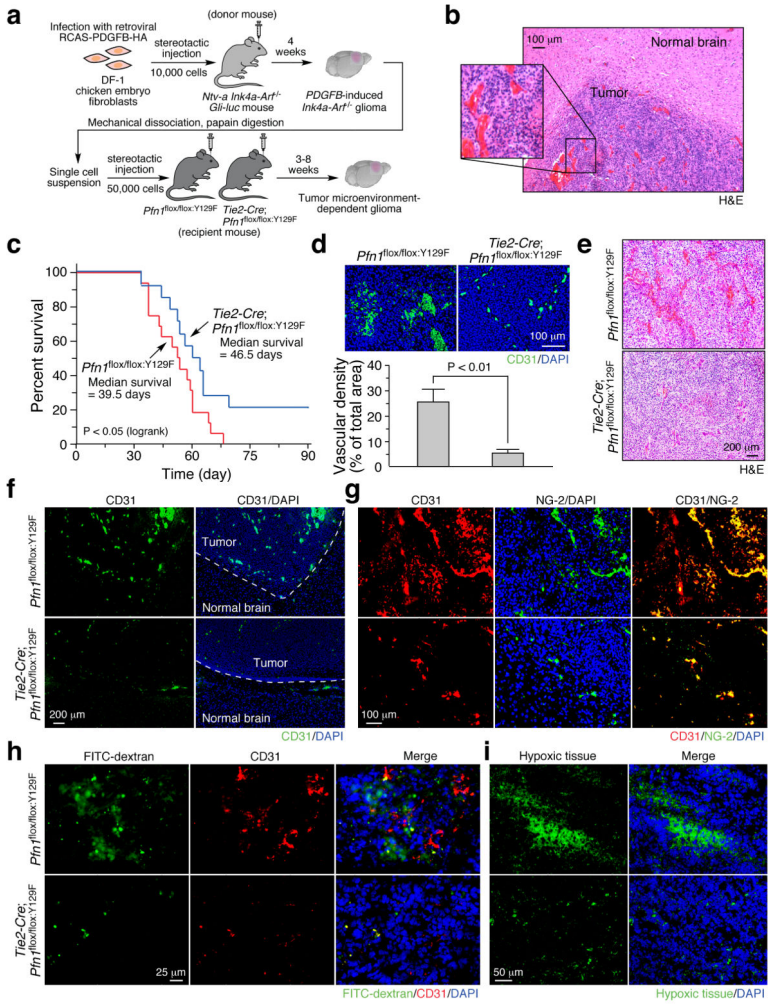

Figure 1.

Pfn-1 phosphorylation at Tyr^{129} in EC induces aberrant vascularization and GBM progression. (**a**) GBM was induced by orthotopic injection of GBM tumor cells, and brain sections subjected to pathological and immunohistochemical analyses. The primary GBM in donor mice is induced by overexpression of PDGF in glial cells through RCAS/tv-a-mediated somatic gene transfer. Recipient mice were had conditional knock-in of *Pfn1*$^{Y129F/Y129F}$ driven by EC-specific *Tie2* promoter. (**b**) Four weeks after tumor cell injection, brains of *Pfn1*$^{flox/flox:Y129F}$ mice were excised and sections subjected to H&E stain. (**c**) Survival was monitored for 90 days post-injection (n = 16 and 14 for *Pfn1*$^{flox/flox:Y129F}$ and *Tie2-Cre; Pfn1*$^{flox/flox:Y129F}$ mice, respectively), and analyzed by two-tailed Logrank test. (**d**) Tumor sections were probed with anti-CD31 antibody. Vascular density was quantified by immunofluorescence (mean ± SEM, n = 9 mice, two-tailed unpaired *t* test). (**e**) Hematoxylin and eosin (H&E)-stained sections. (**f**, **g**) Tumor sections were stained with anti-CD31 and anti-NG-2 antibodies (n = 5 mice). (**h**) Mice were perfused intravenously with FITC-dextran, and EC in tumor sections detected with anti-CD31 antibody (n = 5 mice). (**i**) Mice were injected with Hypoxyprobe-1 (pimonidazole HCl), and

tumor sections probed with monoclonal antibody against pimonidazole adducts and detected with Alexa Fluor 561-conjugated IgG (n = 5 mice).

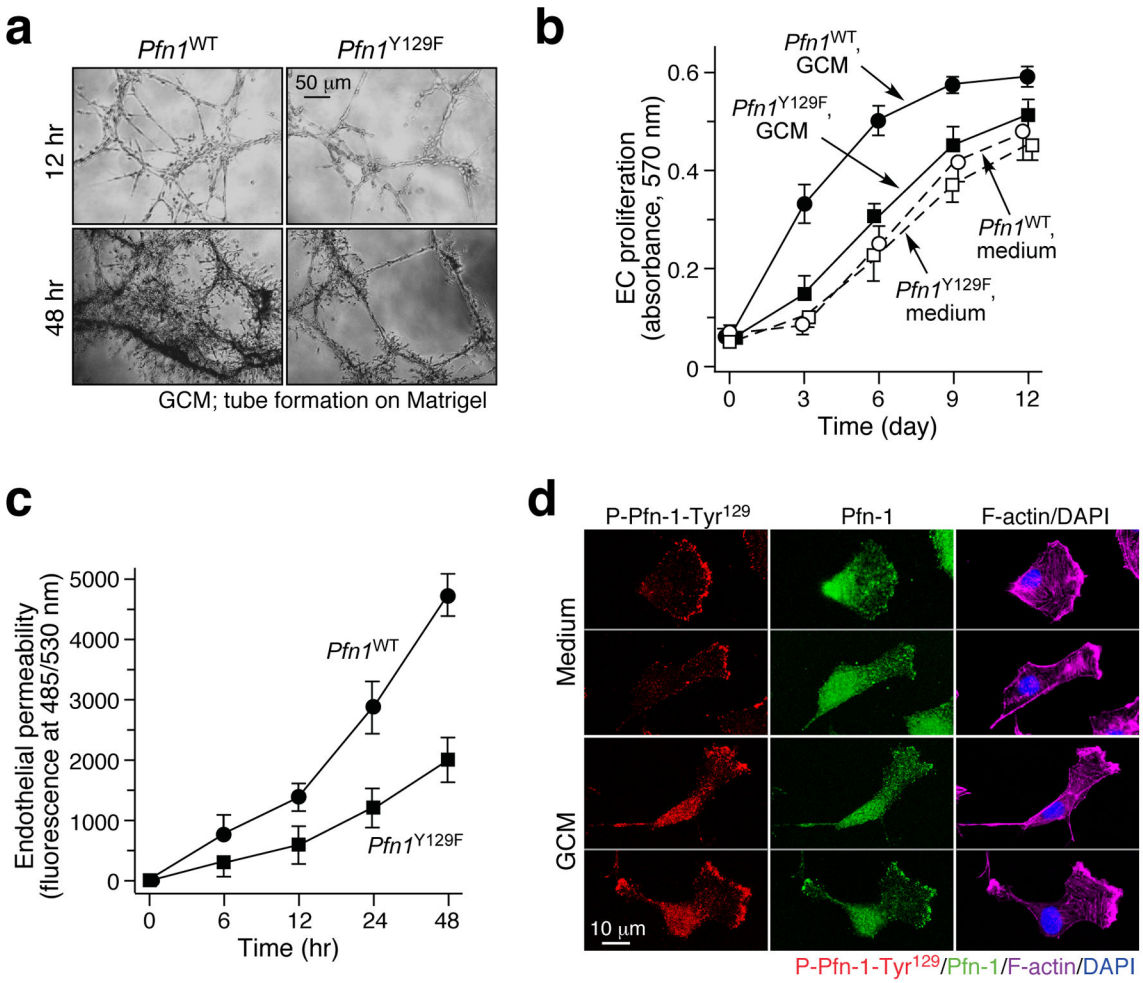

Figure 2.

Pfn-1 phosphorylation at Tyr^{129} is critical for *in vitro* vascular abnormality. (**a**–**c**) EC were isolated from *Pfn1*$^{flox/flox:Y129F}$ (*Pfn1*^{WT}) and *Tie2-Cre; Pfn1*$^{flox/flox:Y129F}$ (*Pfn1*^{Y129F}) mice, and treated with U251 glioma cell-conditioned medium (GCM). (**a**) Tube formation was induced on Matrigel. (**b**) EC proliferation determined by MTT assay (mean ± SEM, n = 5 biologically independent samples per group, one representative experiment shown, and the experiment was repeated 3 times). (**c**) Endothelial monolayer permeability was analyzed by fluorescence of FITC-dextran in transwell plate (mean ± SEM, n = 5 biologically independent samples per group, one representative experiment shown, and the experiment was repeated 3 times). (**d**) Human microvascular EC were treated with GCM, and stained with anti-P-Pfn-1-Tyr^{129} and anti-Pfn-1 antibodies.

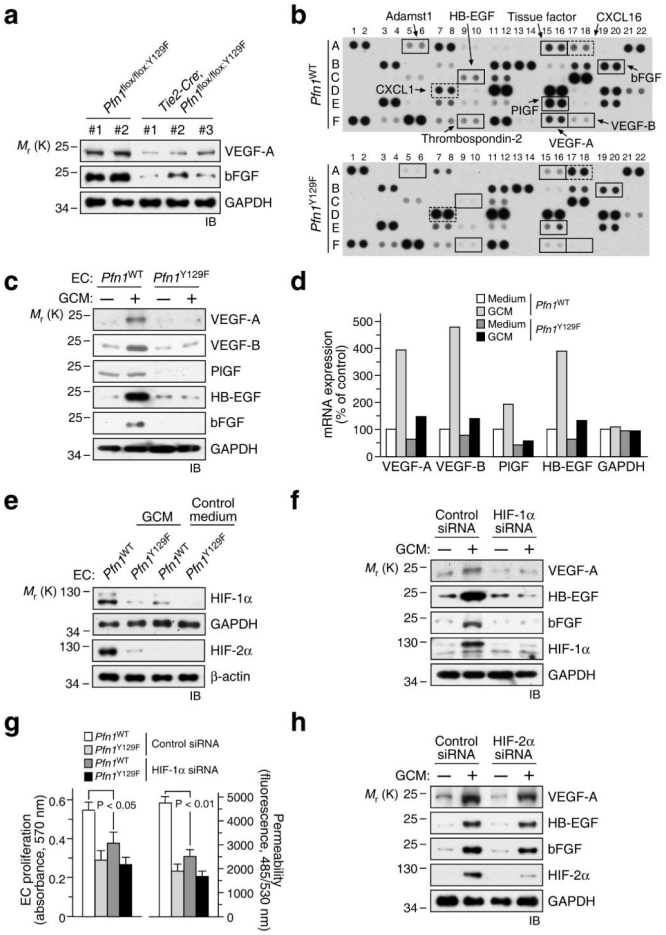

Figure 3.

EC Pfn-1 phosphorylation at Tyr^{129} induces HIF-1α-dependent expression of angiogenic growth factors in glioma microenvironment. (**a**) Tissue lysates from GBM tumors in *Pfn1*$^{flox/flox:Y129F}$ and *Tie2-Cre; Pfn1*$^{flox/flox:Y129F}$ mice were subjected to immunoblot analysis with antibodies described. (**b**–**d**) EC were isolated from *Pfn1*$^{flox/flox:Y129F}$ (*Pfn1*^{WT}) and *Tie2-Cre; Pfn1*$^{flox/flox:Y129F}$ (*Pfn1*^{Y129F}) mice, and treated with U251 glioma cell-conditioned medium (GCM). (**b**) Cell lysates were analyzed with a Mouse Angiogenesis Proteome Profiler Array. (**c**) Cell lysates were subjected to immunoblot analysis. (**d**) mRNA was isolated and analyzed by real-time RT-PCR (mean, 5 technical replicates per group, one representative experiment shown, the experiment was repeated 3 times, two-tailed unpaired *t* test). (**e**) EC were isolated from *Pfn1*$^{flox/flox:Y129F}$ (*Pfn1*^{WT}) and *Tie2-Cre; Pfn1*$^{flox/flox:Y129F}$ (*Pfn1*^{Y129F}) mice, and treated with GCM. Cell lysates were analyzed by immunoblot with anti-HIF-1α and anti-HIF-2α antibodies. (**f**, **g**) EC were transfected with siRNA targeting HIF-1α (or control), and incubated with GCM. (**f**) Cell lysates were subjected to immunoblot analysis. (**g**) EC proliferation and permeability were determined by MTT and transwell assays (mean ± SEM, n = 5 biologically independent samples per group, one representative experiment shown, and the experiment was repeated 3 times, two-tailed unpaired *t* test), respectively. (**h**) EC were transfected with siRNA targeting HIF-2α (or

control), and incubated with GCM. Cell lysates were subjected to immunoblot analysis as shown. Uncropped images of blots are shown in Supplementary Fig. 8.

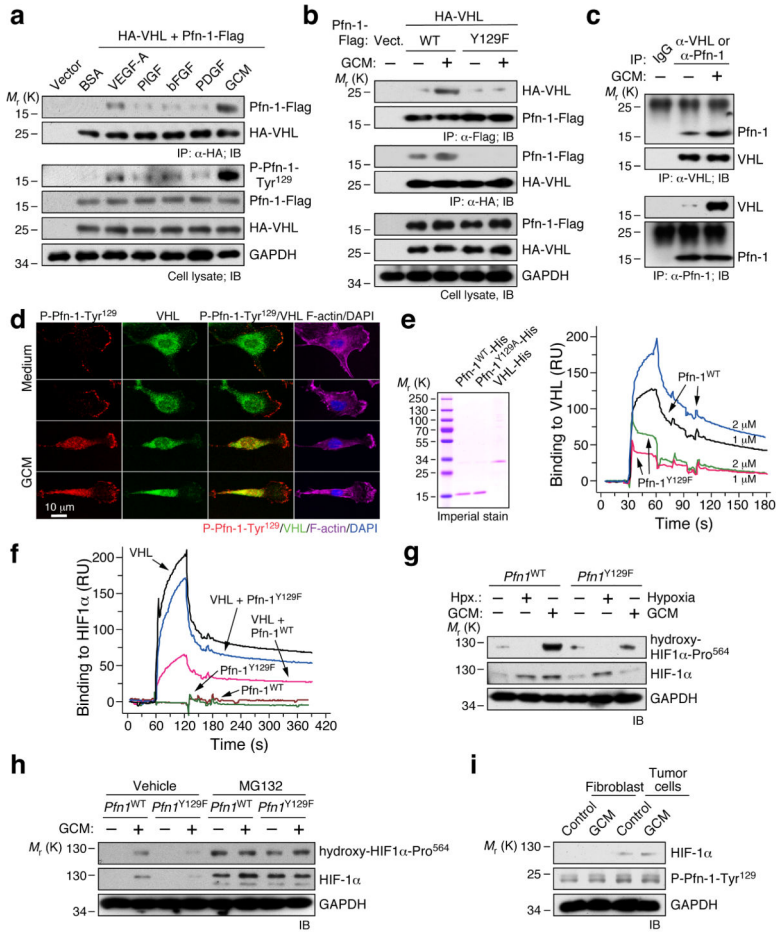

Figure 4.

Tyr^{129}-phosphorylated Pfn-1 increases HIF-1α expression by blocking VHL-mediated degradation. (**a**) Human microvascular EC were transfected with pCMV-HA-VHL plus pcDNA-Pfn-1-Flag constructs (or pcDNA vector control). EC were treated with angiogenic factors or GCM, and lysates immunoprecipitated with anti-HA antibody and subjected to immunoblot analysis. (**b**) EC were transfected with pcDNA (vector), or pCMV-HA-VHL and pcDNA-Pfn-1-Flag with or without Y129F mutation, and treated with GCM as in (**a**). (**c**) EC were treated with GCM. Cell lysates were immunoprecipitated with anti-VHL or anti-Pfn-1 antibody, and subjected to immunoblot analysis as shown. (**d**) EC were treated with GCM and subjected to immunofluorescence analysis. (**e**) Purified Pfn-1^{WT}-His and Pfn-1^{Y129A}-His were *in vitro* phosphorylated with lysate from GCM-treated EC and re-purified with Ni^{+}-beads, and proteins resolved by SDS/PAGE and stained with GelCode blue (left). Pfn-1 interaction with chip-immobilized VHL was determined by SPR (right). (**f**) VHL interaction with immobilized HIF-1α in the presence of Pfn-1^{WT} or Pfn-1^{Y129F} was determined by SPR. (**g**, **h**) EC were isolated from *Pfn1*$^{flox/flox:Y129F}$ (*Pfn1*^{WT}) and *Tie2-Cre; Pfn1*$^{flox/flox:Y129F}$ (*Pfn1*^{Y129F}) mice. EC were (**g**) exposed to hypoxia or treated with GCM, or (**h**) treated with GCM plus 0.1% DMSO (vehicle) or 10 mM MG132, and subjected to immunoblot analysis. (**i**) GBM was induced in *Pfn1*$^{flox/flox:Y129F}$ (*Pfn1*^{WT}) mice, and tumor cells were isolated and cultured. Fibroblasts and tumor cells were treated with glioma-

conditioned medium (GCM), followed by immunoblot analysis. Uncropped images of blots are shown in Supplementary Fig. 8.

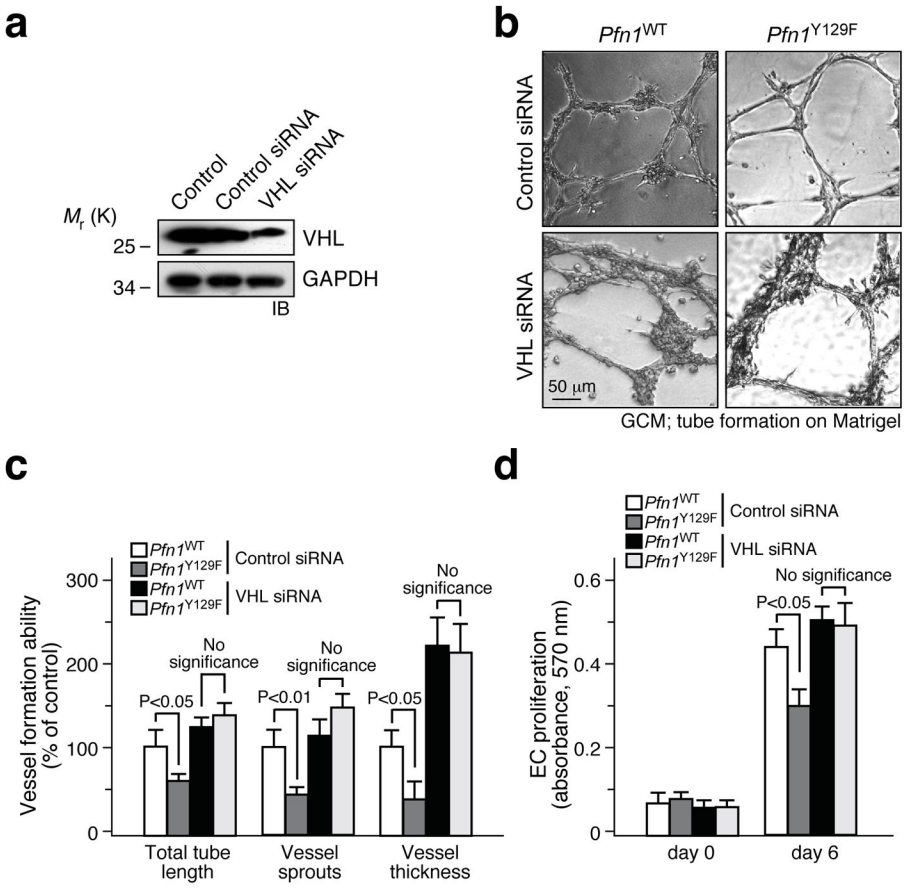

Figure 5.

VHL is critical for Pfn-1 phosphorylation-mediated vascular abnormality. EC were isolated from *Pfn1*$^{flox/flox:Y129F}$ (*Pfn1*^{WT}) and *Tie2-Cre; Pfn1*$^{flox/flox:Y129F}$ (*Pfn1*^{Y129F}) mice and transfected with control or VHL siRNA. (**a**) Cell lysate from *Pfn1*^{WT} EC was resolved by SDS-PAGE and subjected to immunoblot analysis with anti- VHL and anti-GAPDH antibodies. (**b, c**) Tube formation was induced on Matrigel for 24 hr in the presence of glioma- conditioned medium (GCM). (b) Representative images. (c) Total tube length, the number of vessel sprouts, and the thick- ness of vessel walls were quantified (Mean ± SEM, n = 5 biologically independent samples per group, one representative experiment shown, and the experiment was repeated 3 times, two-tailed unpaired *t* test). (**d**) Cells were treated with GCM, and cell proliferation deter- mined by MTT assay (Mean ± SEM, n = 5 biologically independent samples per group, one representative experiment shown, and the experiment was repeated 3 times). Uncropped images of blots are shown in Supplementary Fig. 8.

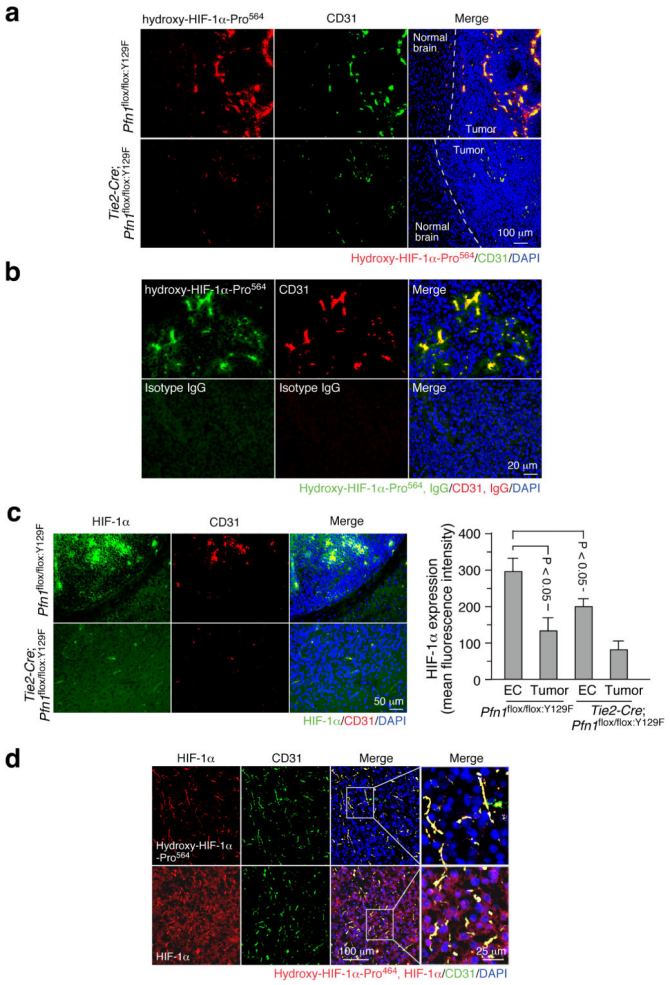

Figure 6.

Expression of HIF-1α and Pro^{564}-hydroxylated HIF-1α in EC of GBM tumor. (**a**–**c**) GBM was induced in *Pfn1*$^{flox/flox:Y129F}$ and *Tie2-Cre; Pfn1*$^{flox/flox:Y129F}$ mice (n = 5 mice). Brain sections were probed with anti-CD31, and (**a**, **b**) anti-hydroxy-HIF-1α-Pro^{564} or (**c**) anti-HIF-1α antibodies, and visualized with Alexa Fluor 488- and Alexa Fluor 561- conjugated second antibodies. (**b**) Brain sections retrieved from GBM tumor in *Pfn1*$^{flox/flox:Y129F}$ mice were probed with anti-CD31 and anti-hydroxy- Pro^{564} or control isotype IgGs. (c) Left, representative images. Right, mean fluorescence intensity was quantified in CD31^{+} EC and tumor area (Mean ± SEM, n = 5 mice, two-tailed unpaired *t* test). (**d**) Brain sections from tumor biopsy specimens of GBM patients (n = 3 samples) were probed with anti-CD31 and -hydroxy-HIF-1α-Pro^{564} or -HIF-1α antibodies.

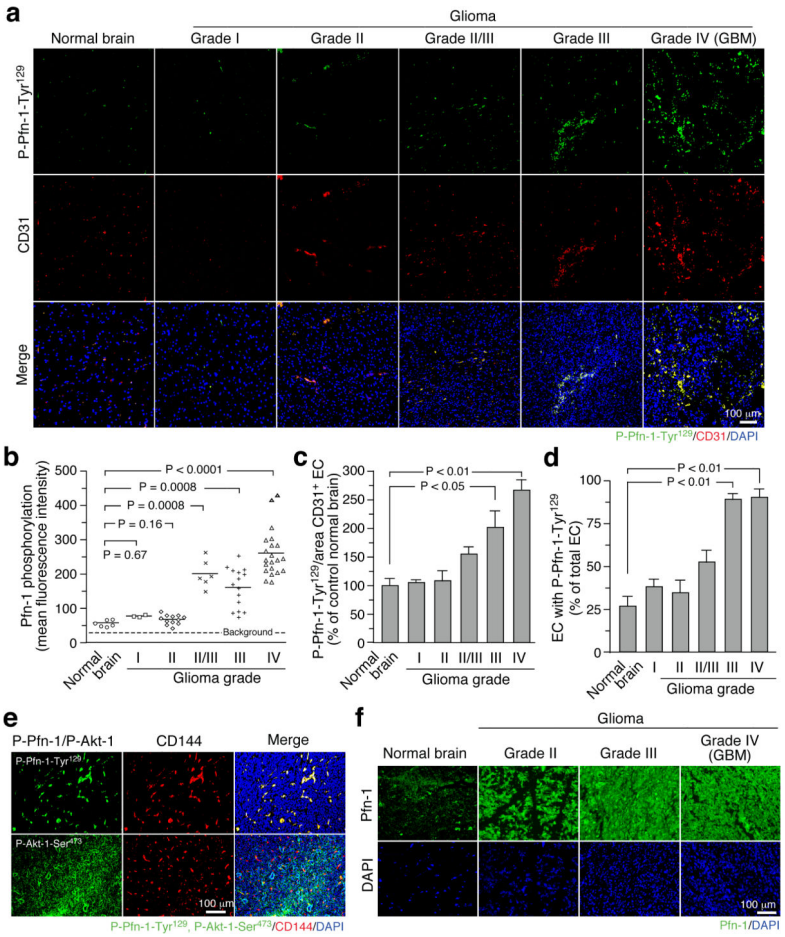

Figure 7.

Increased Tyr^{129} phosphorylation of Pfn-1 in blood vessels of human glioma tumors correlates with grade. (**a**–**d**) Sections from biopsy specimens from subjects with glioma (n = 57 samples, total) and from normal brains (n = 6 samples) were probed with anti-P-Pfn-1-Tyr^{129} and -CD31 antibodies. (**a**) Representative images. (**b**) P-Pfn-1-Tyr^{129} in brain sections from glioma patients or from healthy controls was quantified by immunofluorescence using anti-P-Pfn-1-Tyr^{129} antibody (bars indicate means, total n = 63 samples, two-tailed unpaired *t* test). Background fluorescence detected with omission of primary antibody was subtracted. (**c**) After background subtraction, fluorescence intensity of P-Pfn-1-Tyr^{129} was normalized by area of CD31^{+} EC, and expressed as percentage of control (mean ± SEM, total n = 63 samples, two-tailed unpaired *t* test). (**d**) Quantitative analysis of co-localization of CD31^{+} EC with P-Pfn-1-Tyr129 (mean ± SEM, total n = 63 samples, two-tailed unpaired *t* test). (**e**) Human GBM specimens probed with anti-P-Pfn-1-Tyr^{129}, -CD144 and -P-Akt-Ser^{473} antibodies (n = 5 samples). (**f**) Uniform expression of Pfn-1 in human glioma tumors. Sections from biopsy specimens of human subjects with glioma (n = 4 samples) and from normal brains (n = 5 samples) were probed with anti-Pfn-1 antibodies.

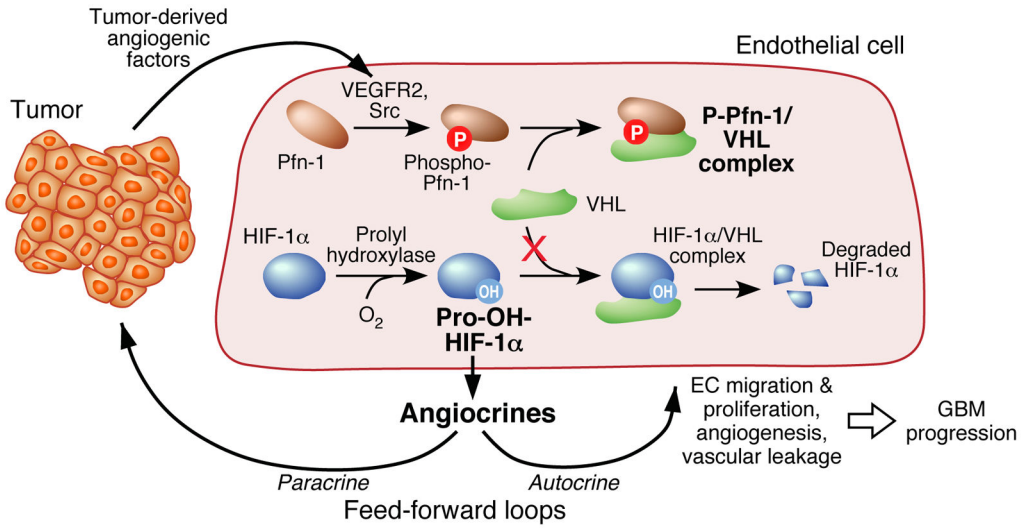

Figure 8.

Schematic illustrating phospho-Pfn-1-mediated induction of HIF-1α driving growth factor production, aberrant vascularization, and GBM progression. The model shows that phospho-Pfn-1 interacts with VHL, prevents VHL-mediated degradation of HIF-1α, and induces accumulation of Pro-hydroxylated HIF-1α in GBM EC with pathological consequences.